COMMISSIONING OF BEAM LOADING COMPENSATION SYSTEM IN THE J-PARC MR

Fumihiko Tamura*, Chihiro Ohmori, Masanobu Yamamoto, Masahito Yoshii, Alexander Schnase, Masahiro Nomura, Makoto Toda, Taihei Shimada, Katsushi Hasegawa, Keigo Hara
J-PARC Center, KEK & JAEA, Tokai-mura, Naka-gun, Ibaraki-ken, Japan 319-1195

Abstract

Beam loading compensation is indispensable to accelerate high intensity proton beams in the J-PARC MR. The MA-loaded rf cavities in the MR are driven by the single harmonic ($h = 9$) rf signals, while the cavity frequency response covers also the neighbor harmonics ($h = 8, 10$). The wake voltage induced by the beam consists of the three harmonics ($h = 8, 9, 10$). We employ the rf feedforward method to compensate the beam loading of these harmonics. The full-digital feedforward system was developed for the MR. We have successfully commissioned the feedforward patterns for all of eight cavities by using high intensity beams with 1.0×10^{14} ppp. We present the commissioning results. The impedance seen by the beam is reduced and the longitudinal oscillations due to the beam loading are reduced. By the beam loading compensation, high power beam operation at the beam power of 200 kW has been achieved.

INTRODUCTION

Beam loading compensation is a key to accelerate high intensity proton beams in the MR of the Japan Proton Accelerator Research Complex (J-PARC).

The parameters of the J-PARC MR and its rf system are listed in Table 1. At present, the MR provides 1.15×10^{14} ppp to the neutrino experiment, which corresponds to the beam power of 230 kW at the repetition period of 2.48 s [1]. The magnetic-alloy (MA) cavities are employed to realize the high accelerating voltage. The maximum rf voltage is 280 kV with 8 cavities. The MR cavities with the Q value of 22 are driven by single harmonic ($h = 9$) rf signals. The frequency response covers not only the frequency sweep of the accelerating harmonic ($h = 9$), from 1.67 to 1.72 MHz, but also the neighbor harmonics ($h = 8, 10$). The wake voltage in the cavity consists of the accelerating harmonic ($h = 9$) and the neighbor harmonics ($h = 8, 10$). A multiharmonic beam loading compensation is important for acceleration of high intensity beams.

We employ the rf feedforward method for the multiharmonic beam loading compensation, like in the J-PARC RCS, in which the impedance seen by the beam is greatly reduced by the feedforward [2]. The function and the architecture of the feedforward system of MR, which are similar to that of the RCS, are described in ref. [3]. The feedforward system works as a tracking bandpass filter, whose passbands at the harmonics ($h = 8, 9, 10$) follow the frequency sweep with programmed gain and phase patterns.

* fumihiko.tamura@j-parc.jp

Table 1: Parameters of the J-PARC MR and its rf system.

circumference	1567.5 m
energy	3–30 GeV
beam intensity	(achieved) 1.15×10^{14} ppp
repetition period (FX)	2.48 s
accelerating frequency	1.67–1.72 MHz
harmonic number	9
number of bunches	8
maximum rf voltage	280 kV
No. of cavities	8
Acc. gaps in a cavity	3
cavity resonant frequency	1.72 MHz
Q-value of rf cavity	22

We report the commissioning results and the effects on the beams.

COMMISSIONING OF FEEDFORWARD

The commissioning of the feedforward system is to adjust the amplitude and phase patterns for the selected harmonics so that the wake voltages are canceled by the feedforward signals. The commissioning methodology which is used for the J-PARC RCS [2] is applied to the MR.

With feedforward, the cavity voltage is the superposition of the driving rf voltage $V_{\mathrm{cav,dr}}(h, t)$, the wake voltage $V_{\mathrm{cav,wake}}(h, t)$, and the feedforward voltage $V_{\mathrm{cav,FF}}(h, t)$, where h is the selected harmonic and t is the time. The superposition is expressed as

$$\begin{aligned} & V_{\mathrm{cav}}(h,t) = \\ & V_{\mathrm{cav,dr}}(h,t) + V_{\mathrm{cav,wake}}(h,t) + V_{\mathrm{cav,FF}}(h,t) \\ & \quad = H_{\mathrm{dr}}^{\mathrm{cav}}(h,t) \cdot V_{\mathrm{dr}}(h,t) + Z'_{\mathrm{cav}}(h,t) \cdot I_{\mathrm{beam}}(h,t) \\ & \qquad + Z_{\mathrm{FF}}(h,t) \cdot I_{\mathrm{beam}}(h,t), \end{aligned} \quad (1)$$

where $V_{\mathrm{dr}}(h, t)$ and $I_{\mathrm{beam}}(h, t)$ are the harmonic components of the LLRF driving rf signal and the beam current, respectively, $H_{\mathrm{dr}}^{\mathrm{cav}}(h, t)$ the transfer function from the LLRF driving rf to the cavity voltage obtained without accelerating a beam, and $Z'_{\mathrm{cav}}(h, t)$ the cavity impedance obtained by accelerating a beam without feedforward. By (1), $Z_{\mathrm{FF}}(h, t)$, which is the transfer function from the beam current to the feedforward gap voltage, is obtained by using the measured voltage and beam current, $V_{\mathrm{cav}}(h, t)$ and

ISBN 978-3-95450-122-9

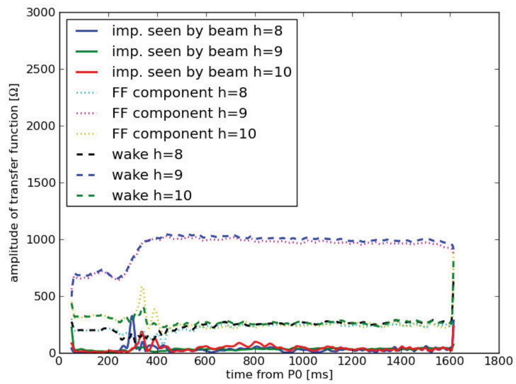

Figure 1: A comparison of the impedances and the feedforward transfer function of cavity #8.

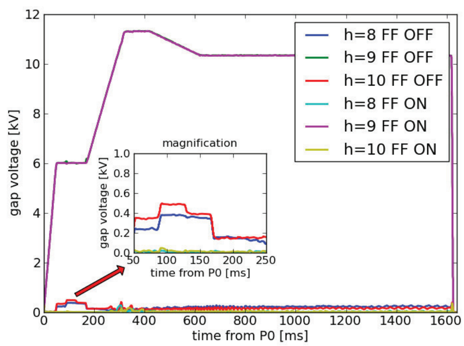

Figure 2: A comparison of the harmonic components of cavity #8 gap voltage without and with feedforward. A magnified plot during injection period is also shown.

$I_{\mathrm{beam}}(h,t)$. The impedance seen by the beam is

$$Z'_{\mathrm{cav}}(h,t) + Z_{\mathrm{FF}}(h,t). \tag{2}$$

Assuming the linear response, the gain and phase patterns are modified to minimize the impedance seen by the beam. Several iterations are necessary to realize the minimum impedance seen by the beam.

The feedforward patterns for all eight rf systems were adjusted using a high intensity beam of 1.0×10^{14} ppp by applying the commissioning methodology described above.

A comparison of the impedances and the feedforward transfer function after the commissioning of cavity #8 is shown in Fig. 1. In the plot, "wake" indicates the impedance seen by the beam without feedforward, "FF component" is the transfer function from the beam current to the feedforward component of the cavity voltage, and "imp. seen by the beam" is the impedance seen by the beam with feedforward.

For the accelerating harmonic ($h = 9$), the amplitude of the feedforward component is close to the impedance

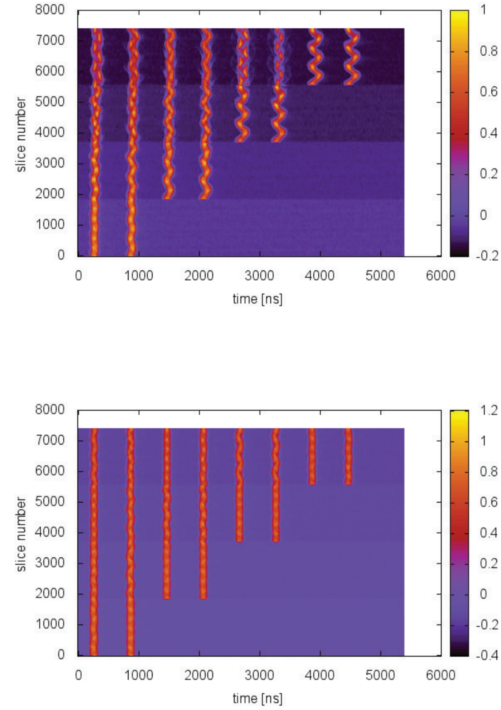

Figure 3: Mountain plots of the WCM signals during the injection period (top) without and (bottom) with feedforward.

seen by the beam without feedforward from injection to extraction, and the impedance seen by the beam with feedforward is low, less than 50 Ω, while the shunt resistance of the gap is 1100 Ω. For the neighbor harmonics ($h = 8, 10$), the errors of the feedforward amplitude are observed from 220 ms to 400 ms and the reductions of the impedances seen by the beam are not so good. Other than that, especially during the injection period where the periodic transient effects are severe, the errors are small and the reductions of the impedance are good.

The harmonic components of cavity #8 gap voltage, without and with feedforward are plotted in Fig. 2. The accelerating harmonic components ($h = 9$) are similar without and with feedforward, because it is controlled strongly by the AVC. The reductions of the neighbor harmonics ($h = 8, 10$) during the injection period are clearly observed.

EFFECTS OF FEEDFORWARD ON THE BEAM

We describe the beam test results with feedforward by using a high intensity beam with 1.0×10^{14} ppp. The feedforward compensation of the neighbor harmonics ($h = 8, 10$) is applied only during the injection period, where the periodic transient effects are severe.

ISBN 978-3-95450-122-9

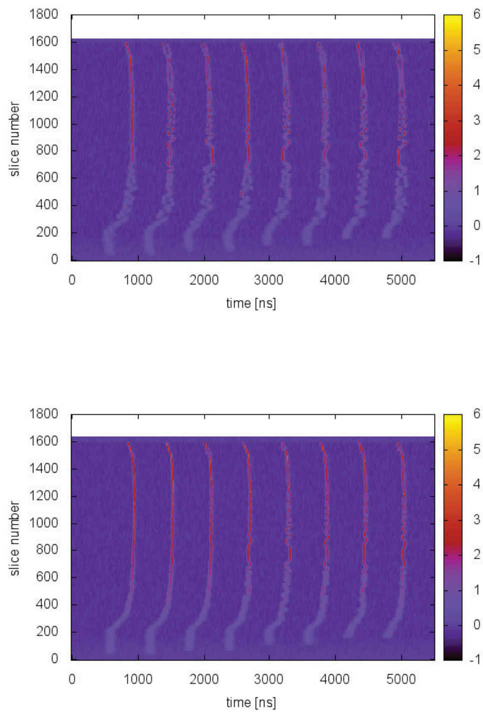

Figure 4: Mountain plots of the WCM signals from injection to extraction (top) without and (bottom) with feedforward.

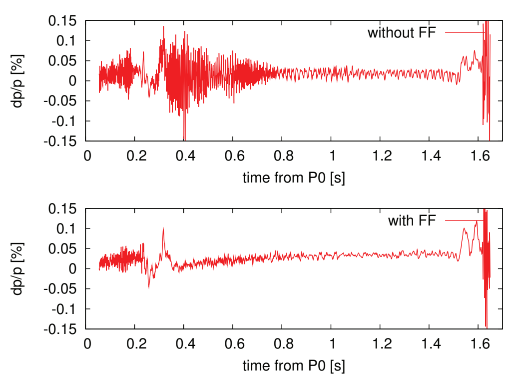

Figure 5: Typical momentum deviation (dp/p) calculated by using the BPM signals (top) without and (bottom) with feedforward.

The mountain plots of the beam signal during the injection period without and with feedforward are shown in Fig. 3. The phase jumps at every injection timing due to the change of the beam loading angle are observed without feedforward. The jumps become larger with accumulated beam and a large amplitude dipole oscillation is observed. The periodic transient effects due to the neighbor harmonics ($h = 8, 10$) are severe when two and four bunches are injected. Without feedforward, the front and rear bunches oscillate differently due to the periodic transient effects.

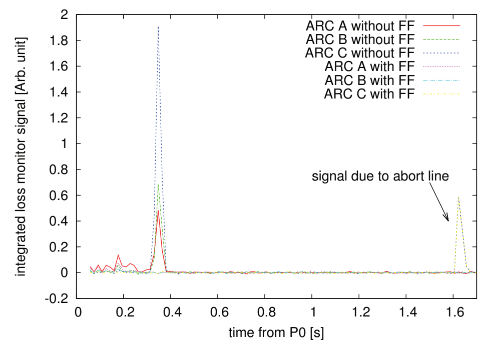

Figure 6: Typical beam loss monitor signal in the arc sections without and with feedforward.

With feedforward, the periodic transient effects are suppressed and the behaviors of the front and rear bunches are similar.

The mountain plots of the beam signal from injection to extraction without and with feedforward are shown in Fig. 4. Without feedforward, the bunches are oscillating throughout the acceleration process. The oscillation starts due to the beam loading during the injection period and it grows from the beginning of the smoothing period of the bending magnet (slice number 220). The momentum deviations of the beam calculated by BPM signals are plotted in Fig. 5. A large momentum oscillation in the order of $\pm 0.1\%$ is observed from 0.3 s to 0.8 s. Beam losses in the arc sections with high dispersion due to the oscillation are observed as shown in Fig. 6. The oscillation is much smaller throughout the acceleration period with feedforward. The beam losses in the arc sections successfully disappear with feedforward.

Thus, for the high power operation of more than 200 kW in the J-PARC MR, the multiharmonic beam loading compensation by the feedforward system is indispensable. The feedforward compensation is used in the normal user operation.

SUMMARY

We developed and commissioned a multiharmonic feedforward system for the J-PARC MR. The impedance seen by the beam is reduced and the longitudinal oscillations due to the beam loading are successfully reduced by the feedforward. The beam loading compensation by the multiharmonic feedforward is indispensable to realize the high power operation in the J-PARC MR. The feedforward compensation is used in the normal user operation.

REFERENCES

[1] T. Koseki et al., Prog. Theor. Exp. Phys. (2012) 02B004

[2] F. Tamura, et al., Phys. Rev. ST Accel. Beams, 14, 051004 (2011).

[3] F. Tamura et al., in Proceedings of IPAC 12, pp. 3915–3917 (2012).